This article was published in

M. Aronniemi, J. Sainio, J. Lahtinen, Chemical state quantification of iron and chromium oxides using XPS: the effect of the background subtraction method, Surface Science 578, 108-123 (2005).

Available online at www.sciencedirect.com
SCIENCE DIRECT®
Surface Science 578 (2005) 108–123
SURFACE SCIENCE
www.elsevier.com/locate/susc

Chemical state quantification of iron and chromium oxides using XPS: the effect of the background subtraction method

M. Aronniemi *, J. Sainio, J. Lahtinen

Laboratory of Physics, Helsinki University of Technology, P.O. Box 1100, FIN-02015 HUT Espoo, Finland

Received 20 October 2004; accepted for publication 16 January 2005
Available online 29 January 2005

Abstract

Quantitative chemical analysis based on X-ray photoelectron spectroscopy (XPS) includes elemental identification and, in many cases, quantification of the chemical states of active surface atoms. The two main parts of the analysis are subtracting the inelastic background and fitting a synthetic lineshape to the data. The analysis of transition metal oxides is typically based on their core level peaks. In the photoelectron spectrum, these regions are usually complicated and therefore the choice of the analysis methods can significantly affect the quantification results. In this work, we studied the chemical state quantification of iron and chromium oxides in the case of two chemical states in both samples; the analysis was based on the 2p region of the photoelectron spectrum. In particular, we focused on the effect of the background subtraction method on the analysis results by using (i) the Tougaard background with Tougaard's universal parameters, (ii) the Tougaard background with Seah's element-specific parameters, and (iii) the traditional Shirley background. The lineshape used to represent the 2p peaks was a Gaussian–Lorentzian product function with a constant-exponential tail. We also characterized typical sources of uncertainty related to XPS-based chemical analysis and compared them to the effect of the background. The chemical state proportions obtained with the studied backgrounds varied by ±5% units for iron oxide and ±3% units in the case of chromium oxide. This background-induced variation was found to be comparable, e.g., to the typical uncertainty in the chemical shift between the states.

Keywords: XPS; Curve fitting; Background subtraction; Iron oxide; Chromium oxide; Chemical state

1. Introduction

In many fields of surface analysis, one of the key questions is the chemical state of the active metal ions of the surface. XPS is typically used in these studies because it is surface sensitive and

* Corresponding author. Tel.: +358 9 451 3132; fax: +358 9 451 3116.
E-mail addresses: mikko.aronniemi@hut.fi, aro@fyslab.hut.fi (M. Aronniemi).

0039-6028/$ - see front matter © 2005 Elsevier B.V. All rights reserved.
doi:10.1016/j.susc.2005.01.019

non-destructive. A reliable quantitative analysis of the chemical states, however, requires a detailed analysis of the photoelectron spectrum. The two main steps of the analysis are subtracting the energy loss background caused by inelastically scattered photoelectrons and resolving the overlapping chemical states. For transition metal oxides, the photoelectron spectrum is typically complex and the analysis turns out to be demanding; on the other hand, transition metal oxides are widely used for many applications. In this paper, we present two case studies concerning the analysis of the 2p region of iron and chromium oxide photoelectron spectra. In particular, we concentrate on the effect of the background subtraction method.

Several background subtraction methods have been proposed in literature. One of the most widely used is the method of Shirley [1], which assumes a constant (energy-independent) probability for energy loss. This leads to a simple, iteratively calculated background in which the background intensity at a given energy is directly proportional to the intrinsic peak area at the high kinetic energy side. The second approach is the formalism of Tougaard [2] which relies on rigorous modeling of inelastic scattering of electrons within a solid. Tougaard has suggested the use of a universal formula for the differential inelastic scattering cross-section with parameters derived from dielectric response calculations. This should be applicable to most metals, their oxides, and alloys provided that they do not have a sharp plasmon structure. A more direct way is to use an experimental energy loss spectrum for determination of the inelastic background [3,4]. Based on REELS measurements of 59 elements, Seah et al. have derived a new set of parameters which can be used in Tougaard's formalism for constructing an element-specific inelastic background [4,5].

The Tougaard method has previously been compared to the Shirley and linear backgrounds in Ref. [6]. In that work, the peak intensities of polycrystalline elemental solids were compared with the theoretical values and the compositions of binary alloys were determined; in addition, the consistency of the results was studied. In Ref. [7], the consistency and validity of these three background subtraction methods were studied as an interlaboratory comparison. In both of these studies, the performance of the Tougaard method was found to be the best. Ro [8] has compared the peak intensities using the linear, Shirley, and Tougaard backgrounds, as well as the electron energy loss deconvolution method. According to his results, these methods showed very similar results. However, except Ref. [9], there has been little discussion on the effect of the background subtraction method on the chemical state quantification.

In this work, we have studied the analysis of the 2p region of iron and chromium oxides with the objective of determining the proportions of the different chemical states of metal ions. The compared background subtraction methods are the Shirley method and the Tougaard method with two sets of parameters: the universal and the element-specific one. The linear background was not considered reasonable for the materials under study. Because the chemical states of both iron and chromium overlap strongly, a peak fitting procedure is necessary for a quantitative analysis. For this purpose, an asymmetric lineshape has been adopted to represent the oxide 2p states, and the effect of its features on the analysis result is also considered.

2. Experimental

The experiments reported in this paper were performed with a Surface Science Instruments SSX-100 ESCA spectrometer using monochromatic AlK_α X-rays and an electrostatic hemispherical analyzer. The spectra were recorded with a pass energy of 50 eV, X-ray spot size of 600 μm, and step size of 0.05 eV or 0.1 eV. Chemical treatments were done in a reactor cell from which the samples could be transferred to the analysis chamber without exposure to the atmosphere. The base pressure in the analysis chamber was around 10^{-9} Torr. A flood gun was used to correct for differential charging when necessary.

For both of the oxides, two types of samples were analyzed: one in which all metal ions have the same chemical state and the other in which there are two states present. The first type of samples served as a reference, whereas the relative

amounts of the two chemical states were determined from the second type, below referred to analyzed sample.

Commercial Fe_2O_3 (hematite) and Fe_3O_4 (magnetite) powders (Strem Chemicals, Inc.) were used as iron oxide samples. Fe_2O_3 served as a Fe^{3+} reference because it contains cations only in the Fe^{3+} state. In addition, it is a stable oxide form and readily available commercially. In bulk Fe_3O_4 33.3% of iron ions are in the Fe^{2+} state and 66.7% in the Fe^{3+} state. Both iron oxide samples were mounted by crushing the powder into an indium foil (Goodfellow, Inc.) under atmosphere. Due to the atmospheric exposure, the sample surfaces contained some adventitious carbon and the surface of Fe_3O_4 powder was to a great extent oxidized to Fe^{3+}. Consequently, Fe_3O_4 powder was sputtered slightly with 4-keV argon ions before the analysis. Fe_2O_3 powder was not sputtered, although it contained some carbon contamination, because the preferential sputtering of oxygen over iron is known to cause reduction. This was highly undesirable because the sample was to be used as a reference. The binding energy scale was shifted to set the oxygen O 1s peak to 530.0 eV.

Commercial Cr_2O_3 powder (Aldrich, Inc.) was used as a reference sample for Cr^{3+}. Also this oxide type is stable and easily available. The analyzed sample was an ALD-grown alumina-supported chromium oxide powder with 13 wt% Cr. According to UV–Vis measurements, 21.3% of chromium was in the Cr^{6+} state and the rest could be assumed to be in the Cr^{3+} state. The photoelectron spectrum was recorded both after calcination (30 min at 600 °C in air) and reduction (15 min at 600 °C in 5% H_2) treatments. Details on the fabrication of the ALD sample are given elsewhere [10]. The binding energies in the chromium oxide spectra were referenced to the alumina Al2p peak at 74.0 eV.

3. Data analysis

The analysis presented here aims to determine the fractions of the chemical states of iron and chromium. We started the analysis of both oxides by recording the spectrum of the reference sample, and after the background subtraction, a set of synthetic peaks was fitted to the data. The parameter values of the reference spectrum fit were then used in the analysis of the spectra consisting of two chemical states. Non-linear least-squares fitting was performed using the Levenberg–Marquardt algorithm. Due to long acquisition times, statistical uncertainty in the spectra was small and the fitting was done in the unweighted way as suggested in Ref. [11].

3.1. Subtraction of inelastic background

The measured spectrum is usually first corrected for the intensity/energy response function (IERF) of the HSA. For our equipment, the exact IERF was not available but an approximate formula was used

$$j(E) = j_0(E) \cdot E^{0.7} \tag{1}$$

where $j_0(E)$ is the measured spectrum at kinetic energy E. The exponent value of 0.7 was a default value given by the manufacturer. Then, a constant line was subtracted from $j(E)$ to set the high kinetic energy side of the peak to zero.

The *Shirley background* [1] is subtracted from the measured spectrum iteratively as

$$F_{k+1}(E) = j(E) - j(E_{\min}) \frac{\int_E^{E_{\max}} F_k(T)\,\mathrm{d}T}{\int_{E_{\min}}^{E_{\max}} F_k(T)\,\mathrm{d}T} \tag{2}$$

where $F_k(E)$ is the background-corrected spectrum after k iterations. The series converges typically after a few iterations and then the background intensity at a given energy is directly proportional to the peak area at the high kinetic energy side. For the Shirley background, the only parameters needed are the endpoints of the range over which it is calculated, i.e. $E_{\min}$ and $E_{\max}$.

Castle and Salvi [12,13] have proposed a modification of the Shirley background in which factor $j(E_{\min})$ is referred to as the shape parameter κ and the integral function is multiplied with a polynomial tail, typically of the first order. The background function is then included in the fitting procedure in order to derive the values for κ and the coefficients of the tail polynome. This approach enables the use of a characteristic back-

ground function for each peak. In order to make the fitting procedure fast enough, one has to be able to express the intrinsic peak area in a closed form instead of calculating it iteratively as is done in the traditional Shirley approach. In our case, the lineshape was complicated, as described below, and its integral could not be expressed in a closed form. For this reason, we decided to use the traditional Shirley background in which the background is subtracted prior to the peak fitting and the κ parameter (or $j(E_{\min})$) is equal for all of the peaks in the analysis region.

The *Tougaard background* correction for a homogeneous and infinite depth distribution (i.e. bulk sample) is calculated as

$$F(E) = j(E) - \lambda_i \int_E^{\infty} j(E')\,K(E'-E)\,\mathrm{d}E' \qquad (3)$$

where λ_i is the inelastic electron mean free path and $K(E'-E)$ is the differential inelastic scattering cross-section [2]. Tougaard et al. have shown that for most metals, their oxides and alloys, the product of the inelastic mean free path and the inelastic scattering cross-section is only weakly dependent on E and can be approximated with a so-called universal formula

$$\lambda_i K(T) = \frac{BT^2}{(C+T^2)^2} \qquad (4)$$

where T is the energy loss in eVs and B and C are parameters [2,14,15]. When constructing the background function, B is a fitting parameter which is adjusted so that $F(E)$ goes to zero in a wide energy range about 30–50 eV below the peak. By fitting function (4) to the calculated dielectric response data, Tougaard has obtained values $B \approx 3000\ \mathrm{eV}^2$ and $C = 1643\ \mathrm{eV}^2$ for homogeneous bulk samples. Although Eq. (3) was derived assuming homogeneous and infinite depth distribution, it can be used for a wide range of depth profiles with reasonable accuracy [16] by scaling B. For materials with a narrow plasmon structure, a three-parameter universal cross-section should be used instead of Eq. (4) [3]. This was not considered necessary for the elements analyzed here.

The advantage of using a Tougaard type background is that the background at a given energy is evaluated using the measured spectrum at higher kinetic energies and is therefore independent of the endpoint selection as long as the spectrum is wide enough so that the correct value for B can be determined. In addition, a Tougaard type background can also be calculated for a shorter spectrum if the values of B and C have been determined earlier using a wider range spectrum.

Seah has proposed [5] that parameters B and C can be replaced with the centroid energy $\overline{E}$ of a single loss function and the exponential slope E_1 of the background. The exponential slope is usually a constant of $E_1 = 714.9$ eV whereas the value of the centroid energy varies between elements. Seah has evaluated the centroid energies for 59 elements from REELS measurements [4]. The dependence of the Tougaard's C parameter on the centroid energy is given by

$$C = \left(\frac{2\overline{E}}{\pi}\right)^2 \qquad (5)$$

and the B parameter is calculated as

$$B = 2C \exp\left(-\frac{\overline{E}}{E_1}\right) \qquad (6)$$

In this approach, C becomes an element-specific parameter and B can again be adjusted in fitting. For iron and chromium, the values reported for C are 756 eV^2 and 806 eV^2, respectively [4].

3.2. Lineshape synthesis and fitting

Ideally, the background subtraction removes completely the contribution of inelastically scattered electrons from the spectrum. However, the intrinsic losses occurring in the emission process can extend to about 50 eV on the low kinetic energy side of a core level peak making it highly asymmetric. In metals, the 2p peaks can be represented by the Doniach–Šunjić (D–S) lineshape [17], which produces a continuous distribution of final states related to the core hole interaction with valence electrons. In practice, the instrumental broadening should be taken into account by convolving the D–S lineshape with a Gaussian resolution function. However, the resulting lineshape cannot be written in a closed form and is thus time-consuming when used as a fitting function.

Compared to the metallic state, the 2p peaks of iron and chromium oxides are wider and have shorter tails. A prominent difference is also the presence of shake-up satellite peaks caused by the configuration interaction due to relaxation of the valence electrons. In the spectrum, they are seen as discrete peaks at the low kinetic energy side of both of the 2p peaks. The separation between the main peak and the satellite is of the order of 6 eV for Fe^{2+}, 8 eV for Fe^{3+}, and 11 eV for Cr^{3+}; Cr^{6+} has no 3d electrons and thus no shake-up satellites. Another characteristic feature of the oxide states is the multiplet splitting. For the 2p states, it is caused by the interaction between the 2p electrons and the unpaired 3d electrons, and it results in a multitude of possible final states. A computational study on the multiplet structure has been presented by Gupta and Sen [18]. For most of these states, however, the energy separation is so small that no discrete peaks will appear with a typical spectrometer resolution. Consequently, the multiplet splitting is seen in the spectrum as asymmetric broadening of the 2p peaks.

For the reasons discussed above, a simple symmetric lineshape does not represent the 2p peaks of iron and chromium oxides satisfactorily. To obtain a proper representation, one possibility is to calculate the final states and broaden them to produce a model spectra. McIntyre and Zetaruk [19] and recently Grosvenor et al. [20] have applied the calculations of Gupta and Sen and fitted the $Fe\,2p_{3/2}$ peak with an envelope of several symmetric peaks. The state structure for iron oxide has been calculated and compared with the experimental XPS data also by Fujii et al. [21] and Droubay and Chambers [22], the latter of whom utilize also X-ray absorption spectroscopy. For chromium oxide, Ünveren et al. have studied the peak structure by combining high-resolution XPS data with XAS measurements [23]. Another approach for a proper representation is to use high-quality reference samples for all of the chemical states and reconstruct the measured spectrum as a linear combination of these empirical lineshapes. This method has been applied to iron oxide by Roosendaal et al. [24] and Graat and Somers [25].

Analysis based on a computational model yields detailed information on the state structure but is laborious and subject to errors in the model. On the other hand, advantages in finding an analytical lineshape that reproduces the reference spectrum are several: the experimental data can be replaced by a set of parameters that are easily transferable, peak fitting with physical constraints becomes possible, and lineshape modifications, e.g. broadening of states, is straightforward. In this work, our aim was to find an analytical lineshape which can reproduce the Fe^{2+}, Fe^{3+}, Cr^{3+}, and Cr^{6+} states and which can be used as a fitting function in a non-linear fitting algorithm. We chose to use a Gaussian–Lorentzian product function with a constant–exponential tail, a lineshape suggested by Sherwood in Ref. [26]. It was used here in a slightly modified form as

$$\mathrm{GL}(E) = \left\{ \left[1 + M \frac{(E_0 - E)^2}{\beta^2} \right] \times \exp\left[(1 - M) \frac{(\ln 2)(E_0 - E)^2}{\beta^2} \right] \right\}^{-1} \tag{7}$$

$$T(E) = c_\mathrm{T} + h_\mathrm{T} \exp\left[-(E_0 - E) \frac{e_\mathrm{T}}{\beta} \right] \tag{8}$$

In the Gaussian–Lorentzian approximation GL(E), E is kinetic energy, E_0 is the peak center, β is a width parameter (approximately 0.5 FWHM), M is the Gauss–Lorentz mixing ratio ranging from 0 for a pure Gaussian to 1 for a pure Lorentzian peak. The asymmetry in the lineshape is produced by the tail $T(E)$ in which c_T determines the height of the constant part, h_T is the height and e_T the slope of the exponential part. Finally, the tail is combined with the peak at the low kinetic energy side to reproduce the total function GLT(E) and the height is determined with parameter h:

$$\mathrm{GLT}(E) \begin{cases} = h\{\mathrm{GL}(E) + [1 - \mathrm{GL}(E)]T\} & \text{for } E < E_0 \\ = h\,\mathrm{GL}(E) & \text{for } E \geqslant E_0 \\ \geqslant 0 & \text{for all } E \end{cases} \tag{9}$$

Two to five such peaks were added up to form a chemical state, and the state was used as a fitting function. The parameters of the component peaks of a given state were given relative to the

parameters of the first peak of the state. This made the fitting procedure easier to control by, e.g., allowing to shift the entire state by changing only one BE value. The lineshape presented above seems to be well suited to represent oxide 2p states subject to strong multiplet splitting as long as the instrumental broadening makes the multiplet states unresolved. A good review of other possible lineshapes has been presented by Fairley [27].

4. Results and discussion

4.1. Iron oxide

4.1.1. Reference spectrum

Fig. 1 represents the Fe 2p region of the recorded Fe^{3+} reference sample after the background has been evaluated using the three different methods, referred to as "Tougaard", "Seah", and "Shirley". The small peak observed at about 704 eV was ascribed to I $3p_{1/2}$ from the indium foil and was not included in the analysis.

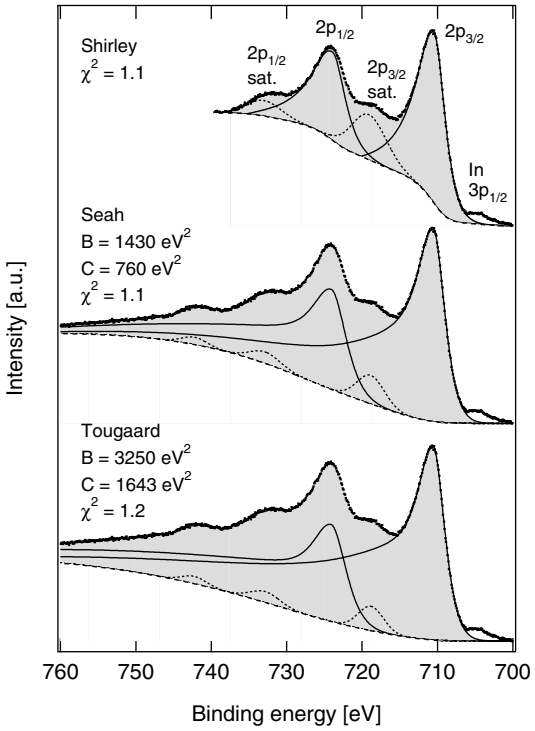

Fig. 1. Curve fits to the Fe 2p region of the reference sample (hematite) after applying three different background subtraction methods. The main peaks are drawn with a solid line, the shake-up satellites with a dotted line, and the background with a dashed line. The shaded area indicates the sum of the component peaks.

For "Tougaard", the background was calculated using the energy range 695–820 eV and a value of 3250 eV^2 was obtained for the B parameter. This is in accordance with the reported bulk value $B \approx 3000$ eV^2. The C parameter was set to the universal value of 1643 eV^2.

For "Seah", the energy range was 695–820 eV and the parameter values were $B = 1430$ eV^2, determined by fitting, and $C = 756$ eV^2, taken from Ref. [4]. The reported bulk value for B is $B = 1424$ eV^2.

In the case of the Shirley background, the parameters to be defined are the endpoints of the background curve. Here the start point was set at the low binding energy side of the $2p_{3/2}$ peak (700 eV) and the end point to the local intensity minimum at the high binding energy side of the $2p_{1/2}$ satellite (740 eV).

Because we did not use any theoretical calculations concerning the lineshapes or peak positions, our fitting strategy was to use as few peaks (i.e. as few fitting parameters) and constrain as few of the parameters as possible. As shown in Fig. 1, the Fe^{3+} state can be reproduced as a sum of $2p_{3/2}$ and $2p_{1/2}$ main peaks and three satellites. The only constraints on the fitting parameters were that the tail parameters and the G/L ratio of the $2p_{1/2}$ main peak had to be equal to those of $2p_{3/2}$ and that the satellites had to be purely Gaussian and without any tail.

The most important spectral parameter values obtained as a result of the fitting are presented in Table 1. It is observed that "Tougaard" and "Seah" give practically equal values but those obtained for "Shirley" deviate to some extent, particularly the binding energy and intensity of the $2p_{3/2}$ satellite. The Fe 2p doublet ratio calculated by Scofield is 0.52 [28], thus the values obtained here are too high. This results from large broadening of the $2p_{1/2}$ component relative to $2p_{3/2}$. The broadening could be explained by the decreased lifetime of the $2p_{1/2}$ hole caused by the Coster–Kronig process [29]. If, however, the broadening was

Table 1
Results of the Fe 2p curve fit

	Fe^{3+}			Fe^{2+}		
	"Tougaard"	"Seah"	"Shirley"	"Tougaard"	"Seah"	"Shirley"
BE $2p_{3/2}$[a] (eV)	710.6	710.6	710.4	709.2	709.2	709.0
$2p_{3/2}$ half width β (eV)	1.9	1.9	1.7	1.5	1.4	1.4
BE $2p_{1/2}$ − BE $2p_{3/2}$ (eV)	13.5	13.5	13.5	13.2	13.1	13.2
$2p_{1/2}$ half width β (eV)	2.4	2.3	2.0	1.5	1.4	1.5
$2p_{1/2}/2p_{3/2}$ intensity ratio	0.59	0.63	0.55	0.47	0.44	0.52
$2p_{3/2}$ satellite shift (eV)	8.2	8.2	8.7	6.0	6.7	5.7
$2p_{3/2}$ satellite intensity	0.04	0.06	0.28	0.02	0.01	0.20
χ^2	1.2	1.1	1.1	2.4	3.5	2.0
Fe^{2+} proportion (%)	–	–	–	32	41	36

The Fe^{3+} values are from the reference spectrum fit and the Fe^{2+} are obtained from the two-state fit to the analyzed spectrum. The width parameter β refers to the width of the low BE side of the $2p_{3/2}$ peak at half maximum. The $2p_{3/2}$ satellite intensity is given relative to the main peak.
[a] Fixed for Fe^{2+}.

constrained to be at most, e.g., 5%, doublet ratios close to the Scofield value were obtained: 0.52 (chi-square 1.9) for "Tougaard", 0.53 (chi-square 1.8) for "Seah", and 0.51 (chi-square 2.0) for "Shirley". On the other hand, because the used lineshape describes the multiplet states only approximately, some of the $2p_{3/2}$ multiplet states may contribute to the $2p_{1/2}$ component. Naturally, it is also possible that the backgrounds remove too little intensity from the $2p_{1/2}$ region compared to the $2p_{3/2}$. When calculating the 2p intensity ratio, a cut-off criterion has to be decided if the measured intensity does not reach the background level within the analyzed binding energy range. This was the case here for the "Tougaard" and "Seah" backgrounds. In this paper, we have set the cut-off point for $2p_{3/2}$ and $2p_{1/2}$ equally far from the respective main peak center. In other words, the integration range was equally wide for both components but shifted by the spin–orbit splitting.

The reduced chi-square values quoted in this paper were evaluated using the typical statistical weighting assuming Poissonian counting statistics. The Q values (the probability of getting a greater chi-square value purely by chance [11]) were less than 0.04 for all the fits, which means that the deviation of the fit from the measured intensity cannot be ascribed to statistical fluctuations only but are mainly due to systematic errors. As pointed out by Cumpson and Seah [11], when the acquisition time is increased enough, systematic errors start to dominate and low Q values are obtained for practically every model.

The origin of the small peak at 742 eV is seldom considered in articles dealing with iron oxide XPS spectra. The first explanation could be that this feature is not from iron at all but is caused by contamination or support material. Taking into account all the peaks in the survey spectrum, no suitable element could be found. Moreover, both the iron oxide powder and the indium support were high-purity (99.999%) materials and sputtering was not observed to affect the peak intensity. Thus, this explanation is considered improbable. Indium and oxygen have no suitable peaks around 742 eV, so we conclude that the feature can be ascribed to iron.

With monochromated AlK_α X-rays there are neither X-ray satellites nor Auger peaks at 742 eV. Consequently, it seems most probable that the feature at 742 eV is a daughter peak of one of the 2p peaks, either of intrinsic type, such as a shake-up satellite, or extrinsic, like a plasmon peak. In both cases, however, there should be such a feature corresponding to both $2p_{3/2}$ and $2p_{1/2}$ peaks. If the parent peak were the $2p_{3/2}$ main peak, we should see the $2p_{3/2}$ counterpart at about 755.5 eV. No such feature is observed, so we end up to ascribe the 742-eV peak to the $2p_{1/2}$ main peak. This means that there should be the $2p_{3/2}$ counterpart at 728.5 eV although no intensity maximum can be observed there.

The possibility of a satellite peak at 728.5 eV was investigated by refitting the spectrum with the ''Tougaard'' background. If no additional constraints were set, refitting produced practically the same result as above (chi-square 1.2, 2p intensity ratio 0.59) and the intensity of the new satellite was negligible. If the broadening of $2p_{1/2}$ was constrained to 5%, the intensity of the new satellite rose to 0.7% of the $2p_{3/2}$ main peak. The chi-square value was 1.7 and the total 2p intensity ratio 0.50 (0.45 for the satellites in total). Above we obtained a chi-square of 1.9 with the same broadening constraint but without the new satellite. A conclusion of these tests is that if the objective is just to minimize the chi-square, it is best achieved without any satellite at 728.5 eV. If in addition it is desirable to get the 2p intensity ratio near the Scofield value, a model with two satellites for both 2p components is reasonable. As our strategy was to fit the data with as few peaks as possible, we decided to omit the possible small satellite at 728.5 eV and use the five-peak representation for the Fe states.

4.1.2. Effect of the background subtraction method

In the analyzed sample (magnetite), iron was present in two states: Fe^{2+} and Fe^{3+}. The background subtraction was done in the same way as for the reference spectrum. The B parameter values obtained were $B = 3220\ eV^2$ for ''Tougaard'' and $B = 1420\ eV^2$ for ''Seah''. In the fitting process, the parameters of the Fe^{3+} state were fixed to the values obtained from the reference spectrum and the binding energy separation between the Fe^{2+} and Fe^{3+} states was fixed to 1.4 eV for the reasons discussed later.

Fig. 2 shows the spectrum of the analyzed sample corresponding to the three studied background removal methods; the most important spectral parameters resulting from the fitting are collected in Table 1. As the result of the state quantification the proportion of Fe^{2+} is quoted here. This was 32% for ''Tougaard'', 41% for ''Seah'', and 36% for ''Shirley''. The stoichiometric bulk value for the proportion of Fe^{2+} in Fe_3O_4 is 33%, but it is possible that the sputtering performed before the XPS measurement changed the surface stoichiometry. For both the states, the integration for area

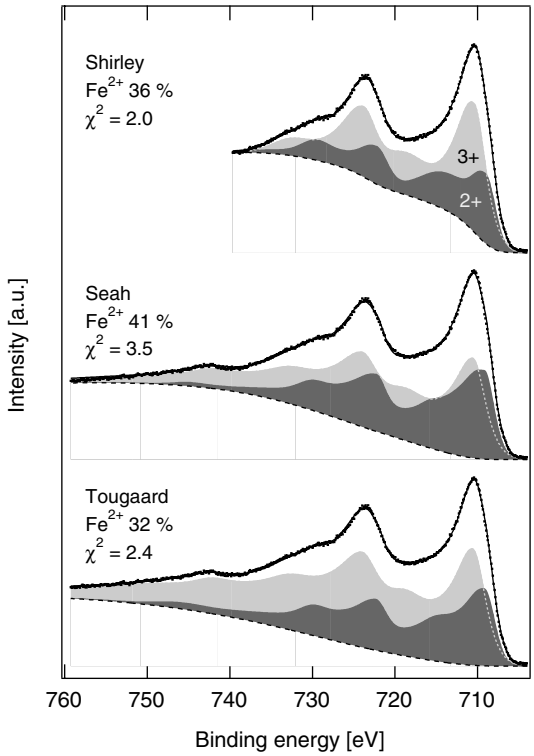

Fig. 2. Decomposition of the Fe2p region of the analyzed sample (magnetite) after subtracting the three backgrounds. The solid line presents the sum of the two states.

calculation was performed equally far from the $2p_{3/2}$ peak of the state.

The chi-square values for the analyzed spectrum fits are slightly greater than those for the reference spectrum. This means either that the applied peak shape (with the assumptions made) cannot reproduce the Fe^{2+} state as well as the Fe^{3+} state or that the used background subtraction methods do not remove the inelastic background consistently for the two spectra.

The choice of the background parameters should be considered carefully. For Tougaard-type backgrounds, the criterion for the B parameter may be inconvenient if there are interfering peaks in the region where the background should follow the experimental measured spectrum. For the Shirley background, the choice of the endpoints affects the background shape, and this causes error in particular if the statistical fluctuation in the spectrum is high (low intensity level). In this work,

we characterized these errors by constructing backgrounds with several parameter values. It was observed that for the iron oxide spectra, having the maximum intensity of about 500 kcounts/eV, this type of error in the Fe^{2+} proportion was less than ±2% units for all the backgrounds.

The effect of random error in the data (electron counting statistics) was studied by Monte Carlo simulation. Two hundred spectra were simulated by generating random noise to the function fitted to the measured spectrum. For a given data point with N counts, the distribution of noise was assumed to be Gaussian with a mean of zero and variance of N. After generating the spectra, the Fe^{2+} and Fe^{3+} states were fitted to them. The standard deviation of the obtained Fe^{2+} proportions was 0.5% units. The sensitivity of the fitting algorithm to the initial guess of the parameter values led typically to uncertainty of less than ±0.3% units. However, this type of uncertainty tends to increase when the number of free fitting parameters is increased.

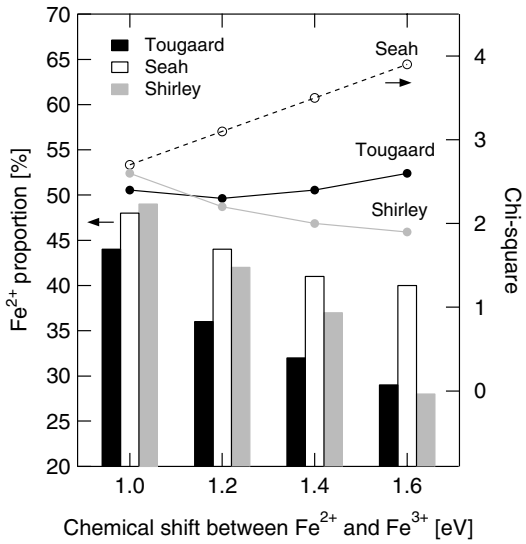

Fig. 3. Fe^{2+} proportion as a function of the chemical shift (binding energy separation) between the Fe^{2+} and Fe^{3+} states. The Fe $2p_{3/2}$ binding energy was held at the value obtained from the reference spectrum (see Fig. 4).

4.1.3. Effect of the lineshape and energy range

After studying the background-induced variation in the state quantification results, we wanted to compare it with the systematic errors associated with the curve fitting. In the case of the 2p region of iron oxide, three sources of systematic error were considered particularly important: the assumed binding energy separation between the Fe^{2+} and Fe^{3+} states, the binding energy scale referencing, and the width of the analyzed energy range. A comprehensive general review of the systematic errors in XPS has been presented by Powell and Seah [30].

Due to the strong overlap between the Fe^{2+} and Fe^{3+} states, the peak fitting is sensitive to the binding energy separation (i.e. the chemical shift) between these two states. The values reported in the literature range from 1 eV to about 2 eV, see e.g. Refs. [21,25,31]. Fig. 3 illustrates the effect of the chemical shift on the proportion of Fe^{2+} for the studied background subtraction methods. It is observed that when the chemical shift increases from 1.0 eV to 1.6 eV, the Fe^{2+} proportion decreases by 15% units for "Tougaard", 8% units for "Seah", and 21% units for "Shirley". For a given chemical shift value, the background-induced difference in the Fe^{2+} proportion is 5–11% units. For "Shirley", the chemical shift values greater than 1.6 eV resulted in unphysically high satellite peak intensities. No such chemical shift value was found that would have minimized the chi-square for all the three methods. As a compromise, 1.4 eV was chosen in the previous section for the comparison of the background subtraction methods. The results show that the effect of uncertainty of the chemical shift is typically comparable to that of the background choice.

Another potential source of error is the binding energy of the Fe $2p_{3/2}$ peak. For iron oxides, the oxide O 1s or the adventitious carbon C 1s peak is normally used as a binding energy reference, and the error in the Fe $2p_{3/2}$ position typically related to this procedure is 0.1–0.2 eV. Fig. 4 presents the Fe^{2+} proportion as a function of the Fe $2p_{3/2}$ peak position. Now the difference between the minimum and maximum proportions is 8% units for "Tougaard", 3% units for "Seah", and 7% units for "Shirley". The effect of the background choice for a given peak position value is 6–11% units. Note that in this case, the chi-square

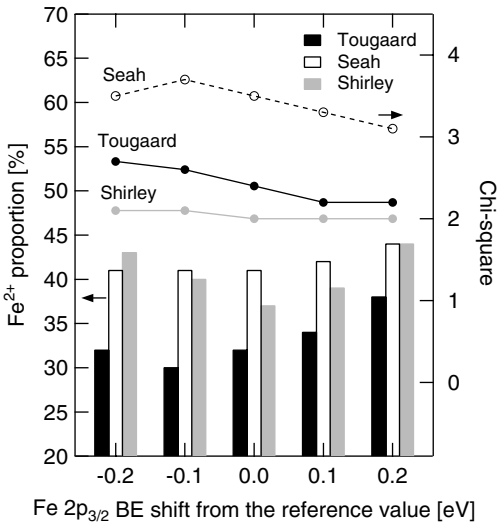

Fig. 4. Fe^{2+} proportion as a function of the Fe $2p_{3/2}$ binding energy of the Fe^{3+} state. A value of 0 eV on the abscissa refers to the case in which the peak is set to the location given by the reference spectrum.

shows only tiny variation between the fits, so it does not serve as a good indicator of the correct peak location.

One of the most common ways to quantify the chemical states of the transition metal oxides is to analyze the $2p_{3/2}$ peak, use the Shirley background, and represent the chemical states with symmetric G–L peaks. Because the states of iron overlap strongly, the binding energies of the states can be considered as the minimum input information required. We compared this simple approach to the procedure described above. When the Fe^{3+} binding energy was derived from the reference spectrum (refitted with a symmetric G–L peak) and the state separation was set to 1.4 eV, the analysis gave a Fe^{2+} proportion of 15% with a chi-square of 17. The obtained proportion is significantly less than the 36% determined above and the large chi-square value indicates a poor correspondence with the data. Reliability of this short-range analysis can be improved by fixing also the width and the G/L ratio of the Fe^{3+} state to the reference values. This approach gave 32% for the Fe^{2+} proportion but an even larger chi-square value of 52.

Because these results show that the simple symmetric lineshape fails to fit to the data properly, it was reasonable to fit an asymmetric peak to the $2p_{3/2}$ region. We used again the reference spectrum to fix the parameter values of Fe^{3+} and constrained the binding energy separation between the states to 1.4 eV. The resulting Fe^{2+} proportion was 44% with a chi-square of 2.6. Thus, the quality of the fit was considerably better than for the symmetric lineshape but the analysis result differs still from that obtained by analyzing the full 2p region.

4.2. Chromium oxide

4.2.1. Reference spectrum

Fig. 5 shows the fitting results of the Cr^{3+} reference spectrum after the background has been subtracted with the three studied methods. For "Tougaard" and "Seah", the *B* parameter was determined by setting the background curve to follow the data at 660–695 eV (not shown in Fig. 5).

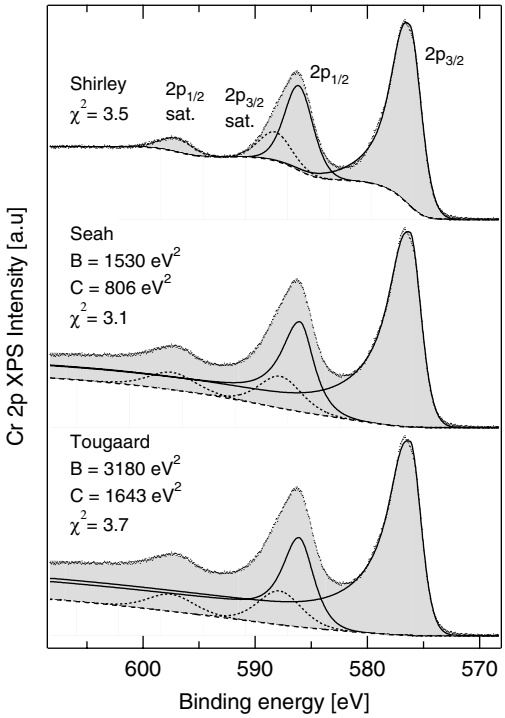

Fig. 5. Curve fits to the Cr 2p region of the Cr^{3+} reference sample after applying the three background subtraction methods. The main peaks are drawn with solid line, the shake-up satellites with dotted line, and the background with dashed line. The shaded area indicates the sum of the component peaks.

This gave $B = 3180\ \mathrm{eV}^2$ for "Tougaard" and $B = 1530\ \mathrm{eV}^2$ for "Seah"; both of these are slightly higher than the reported bulk values $B \approx 3000\ \mathrm{eV}^2$ and $B = 1514\ \mathrm{eV}^2$. For the C parameter, the values were $C = 1643\ \mathrm{eV}^2$ for "Tougaard" and $C = 806\ \mathrm{eV}^2$ for "Seah". The Shirley background was calculated piecewise at 570–595 eV and 595–605 eV. Otherwise the background would have exceeded the measured intensity between the $2p_{1/2}$ peak and its satellite.

Table 2 shows the most important parameters obtained from the fitting. Again the broadening of the $2p_{1/2}$ peak relative to the $2p_{1/2}$ peak was allowed. For "Tougaard" and "Seah", the doublet ratio is close to the value of 0.52 calculated by Scofield [28] whereas the "Shirley" value is clearly lower. The fit made after the "Seah" background subtraction gave the lowest chi-square value. Again, the Q values of the fits were practically zero indicating that systematic uncertainty dominates.

4.2.2. Effect of the background subtraction method

Fig. 6 shows the fitting results of the analyzed chromium oxide sample (ALD-grown alumina-supported catalyst) after the calcination treatment. It was assumed that chromium was present in the two main oxidation states: Cr^{3+} and Cr^{6+}. The B parameter values were $B = 1100\ \mathrm{eV}^2$ for "Tougaard" and $B = 800\ \mathrm{eV}^2$ for "Seah". These values are lower than for those of the bulk reference sample, which indicates that the chromium layer in the analyzed sample was thinner. Knowing the ALD fabrication method, this was to be expected. The

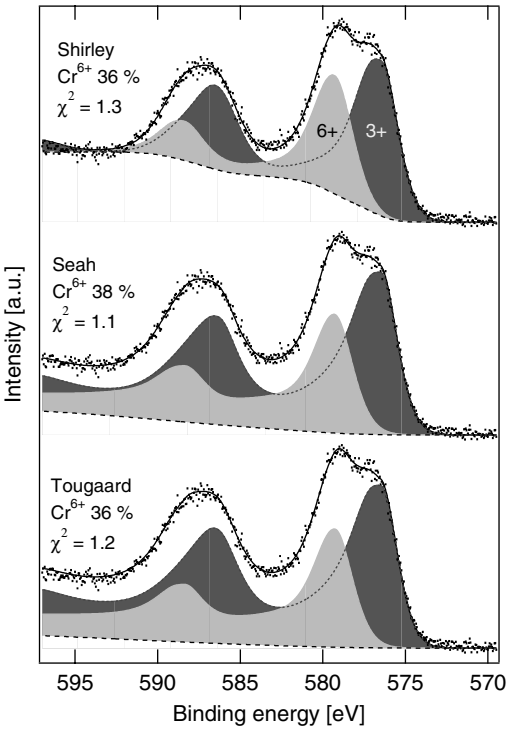

Fig. 6. Decomposition of the Cr 2p region of the analyzed chromium oxide sample after the calcination. The solid line presents the sum of the two states.

Table 2
Results of the Cr 2p curve fit

	Cr^{3+}			Cr^{6+}		
	"Tougaard"	"Seah"	"Shirley"	"Tougaard"	"Seah"	"Shirley"
BE $2p_{3/2}$[a] (eV)	576.5	576.5	576.5	579.3	579.3	579.3
$2p_{3/2}$ half width β (eV)	1.2	1.2	1.3	1.3	1.3	1.3
BE $2p_{1/2}$ – BE $2p_{3/2}$ (eV)	9.9	9.8	9.9	9.1	9.1	9.1
$2p_{1/2}$ half width β (eV)	1.6	1.5	1.6	1.3	1.3	1.4
$2p_{1/2}/2p_{3/2}$ intensity ratio	0.54	0.55	0.40	0.49	0.32	0.28
$2p_{3/2}$ satellite shift (eV)	11.6	11.5	12.0	–	–	–
$2p_{3/2}$ satellite intensity	0.15	0.14	0.14	–[b]	–	–
χ^2	3.7	3.1	3.5	1.2	1.1	1.3
Cr^{6+} proportion (%)	–	–	–	36	38	36

The Cr^{3+} values are from the reference spectrum fit and the Cr^{6+} parameters are obtained from the two-state fit to the analyzed spectrum recorded after the calcination. The width parameter β refers to the width of the low BE side of the $2p_{3/2}$ peak at half maximum. The $2p_{3/2}$ satellite intensity is given relative to the main peak.

[a] Fixed for Cr^{6+}.

[b] Cr^{6+} has no satellites

results of the two-state fit are collected in Table 2. The binding energy of the $2p_{3/2}$ peak was allowed to vary in the fitting but the separation between the Cr^{3+} and Cr^{6+} was fixed to 2.8 eV. In all the cases the $2p_{3/2}$ peak of Cr^{3+} settled at 576.5 eV which agrees well with the reference spectrum and literature. From Fig. 6 it is observed that the applied lineshape reproduces the two chemical states with low chi-square values. The proportion of the Cr^{6+} state was 36–38% for all the backgrounds. The variation in the Cr^{6+} proportion caused by the uncertainty in the background parameters was ±3% units (maximum 2p intensity 100 kcounts/eV) whereas the statistical fluctuation in the data resulted in a standard deviation of 0.8% units (Monte Carlo simulation with 200 spectra).

Thus, all the methods give practically the same result although variation is observed in some spectral parameters, e.g. the $2p_{1/2}/2p_{3/2}$ intensity ratio. It is somewhat unexpected that the result obtained after the Shirley background subtraction does not deviate from the others although the depth distribution in the analyzed sample was different from that of the reference sample.

From Fig. 6 it is observed that the fitting procedure makes the Cr^{6+} state asymmetric and broadens the $2p_{1/2}$ peak compared to the $2p_{3/2}$ peak. However, in the Cr^{6+} state there are no free or unpaired 3d electrons, and so there should be neither multiplet splitting causing asymmetry nor Coster–Kronig transition causing $2p_{1/2}$ broadening. If the 2p peaks of Cr^{6+} are constrained symmetric and the widths of the $2p_{1/2}$ and $2p_{3/2}$ peaks equal, the result for both "Tougaard" and "Seah" is 40% which is only slightly greater than that obtained above. The chi-square value of 1.8 indicates worse agreement with the data compared to the values of 1.2 and 1.1 above. With the Shirley background no acceptable fit could be obtained with symmetric and equally wide peaks.

As the second case for chromium oxide we analyzed the same sample after the reduction treatment which is expected to decrease the fraction of Cr^{6+}. The background subtraction was carried out with the same parameters as above and all the parameters except the Cr^{3+} binding energy were fixed to the values used above. Fig. 8 shows the analysis results corresponding to the three background subtractions. It is now observed that according to "Tougaard" and "Seah", Cr is within the uncertainty of the analysis completely (>98%) reduced to Cr^{3+}, whereas "Shirley" gives 7% for Cr^{6+}. Thus, in the limit of low concentrations, the effect of the background choice can be significant.

4.2.3. Effect of the lineshape and energy range

When it comes to the sources of systematic error, the energy separation between the two states was again considered to have the strongest impact. The effect of this parameter on the analysis of the calcined sample has been studied in Fig. 7. It is observed that the variation in the Cr^{6+} proportion is small and the chi-square is minimized at 2.8 eV.

In order to see the effect of limiting the analysis to the $2p_{3/2}$ peak instead of the full 2p region, the Shirley background subtraction and the three short-range analyses applied above for iron oxide (Section 4.1.3) were performed for the calcined sample. The results were

- symmetric lineshape, no parameters fixed: Cr^{6+} 53%, chi-square 1.1;

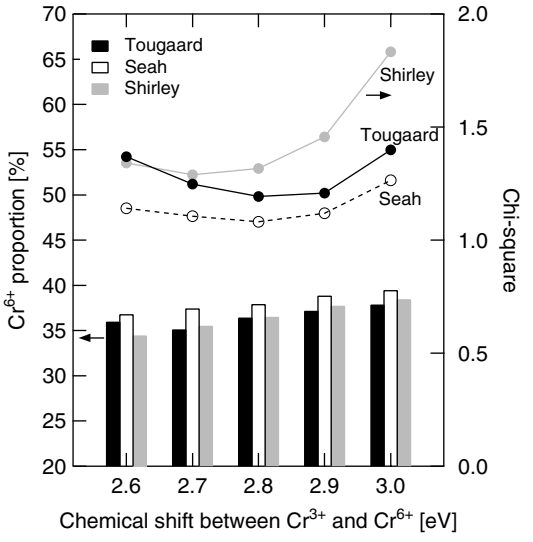

Fig. 7. Cr^{6+} proportion as a function of the chemical shift (binding energy separation) between the Cr^{3+} and Cr^{6+} states determined by the three background subtraction methods.

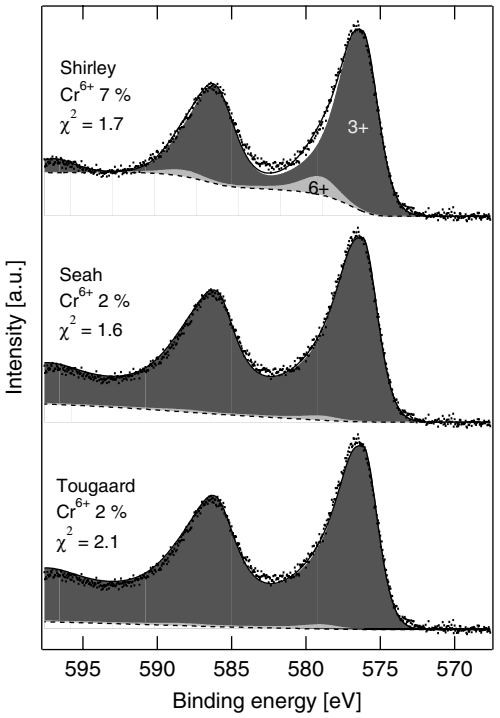

Fig. 8. Decomposition of the Cr 2p region of the analyzed chromium oxide sample after the reduction. The solid line presents the sum of the two states.

- symmetric lineshape, Cr^{3+} parameters from the reference spectrum: Cr^{6+} 38%, chi-square 1.7;
- asymmetric lineshape, Cr^{3+} parameters from the reference spectrum: Cr^{6+} 41%, chi-square 1.1.

When analyzing the $2p_{3/2}$ region only, the $2p_{3/2}$ satellite of Cr^{3+} does not contribute to the state area, whereas the intensity of the Cr^{6+} state, lacking satellites, is completely included. Assuming that the intensity of the $2p_{3/2}$ satellite is 15% of the main peak intensity, the above-mentioned short-range analyses give 49%, 35%, and 38%. The proportion of Cr^{6+} obtained by analyzing the full 2p region was 36% with a chi-square of 1.3 (the "Shirley" case in Section 4.2.2).

4.3. Discussion

Both in the case of iron and chromium oxide, the reference sample had a layer of adventitious carbon on top of it whereas the analyzed samples were free of carbon. Thus, the inelastic background of the reference sample was somewhat different from that of the analyzed sample. For iron oxide, the reference sample was not sputtered in order to avoid the reduction of Fe^{3+} caused by preferential sputtering. However, for the analyzed sample sputtering was necessary to remove the oxidized surface layer, and preferential sputtering was not considered harmful. For chromium oxide, sputtering of the reference sample seemed to cause charging problems and distortion of the spectral features, so it was avoided. The analyzed sample was calcined before the measurement and the calcination removed the carbon contamination.

When a carbon overlayer is present, the sample is not homogeneous and Eq. (3) is not exact. The effect of an overlayer can be included in the background applying the detailed analysis presented by Tougaard [32,33]. However, we wanted to keep the analysis presented here simple and applied Eqs. (3) and (4) with the B parameter adjusted with respect to the changes in the inelastic background. This approach has been shown to be a reasonable approximation for different classes of in-depth concentration profiles [16]. In our case, the Fe^{2+} and Cr^{6+} proportions obtained after taking the carbon overlayer into account using the QUASES software [33] were of the order of 1% unit higher compared with the approximative method. However, when the overlayer thickness increases, all the three backgrounds considered here will probably fail to remove the background intensity properly.

Another potential source of error in the background subtraction was the assumption that the ratio of the two chemical states was constant with respect to the depth. If reasonable assumptions of the in-depth distribution can be made and bulk reference spectra are available for all the chemical states considered, the QUASES software [33] can be used to do the quantification as a function of depth as shown, e.g., by Grosvenor et al. [20]. The in-depth distribution of the chemical states can also be determined using angle-resolved XPS. An example of this approach can be found, e.g., in Ref. [34].

As shown above, the procedure presented here can be used to obtain good-quality fits to experimental 2p spectra of iron and chromium oxides provided that the instrumental resolution makes the multiplet states unresolved. However, to confirm the physical validity of the fits and to see which background works best, we should know the true fractions of Fe^{2+} and Cr^{6+} in the analyzed samples. Because we did not want to use reference samples for Fe^{2+} and Cr^{6+}, most of their parameters were set free in the fitting process. If the resulting lineshape deviates from the true one, error may be induced in the quantification. In particular, we have assumed that both states in both materials can be represented by the same function form (Eqs. (7)–(9)). We know that this is not exact because the 2p states are actually splitted into several components due to, e.g., multiplet splitting as described by Gupta and Sen [18] and that there is also likely to be shakeup structure in the 0–10 eV energy range below the peaks which is not accounted for by the smooth functions in Eqs. (7)–(9). For the reference states our results show that the true peak envelope can be reasonably approximated with the assumed lineshape, but for the states without reference sample we, of course, cannot be sure. If the lineshape of these states were considerably different, e.g. contained more structure, the analysis results would probably change as well.

One possibility to check the validity of the states obtained by fitting would be to analyze a series of spectra using the same set of parameter values for each of the states in each spectrum. The ability to reproduce the series is a natural criterion for a good state representation. Target factor analysis (TFA) provides a convenient means to analyze a series of spectra, see e.g. [35]. In this case, the states obtained by fitting the first spectrum would be as the factors and the algorithm would find the coefficients (loadings) that reproduce the rest of the spectra best.

5. Conclusions

The 2p region of the photoelectron spectra of iron and chromium oxides is rich in features and this makes the chemical quantification demanding. The spectra consist of asymmetric peaks, shake-up satellites, and high intrinsic background. In the present work, we have used three different background subtraction methods and a simple asymmetric lineshape to reproduce the chemical states of iron and chromium. In the analyzed samples, cations were present in two chemical states, Fe^{2+} and Fe^{3+} for iron and Cr^{3+} and Cr^{6+} for chromium, and a quantification procedure was carried out to determine their relative amounts. Reference samples were used for Fe^{3+} and Cr^{3+} and the other states were fitted to the data.

The objective of this work was to find out the effect of the background subtraction method on the quantitative chemical analysis. The compared backgrounds were the Tougaard background with Tougaard's universal parameters (''Tougaard''), the Tougaard background with Seah's element-specific parameters (''Seah''), and the traditional Shirley background (''Shirley''). In the case of iron oxide, the proportion of Fe^{2+} was quantified, and the effect of the background choice was observed to be of the order of ±5% units. Typically the highest proportion was obtained with ''Seah'' and lowest with ''Tougaard''. For chromium oxide, the proportions of Cr^{6+} obtained using the three backgrounds fell within ±3% units. In the limit of small proportion (reduced chromium oxide sample), the analysis result was qualitatively different: ''Shirley'' suggested that some of the chromium was left in the Cr^{6+} state while the complete reduction into Cr^{3+} could be deduced with ''Tougaard'' and ''Seah''.

The effect of the background choice was compared to other sources of uncertainty. Of these sources the statistical fluctuation in the data, the choice of the background parameter values, and the assumptions made on the spectral parameters were included in the comparison. By Monte Carlo simulations it was observed that the statistical fluctuation in our data caused a standard deviation of less than 1% unit for the Fe^{2+} and Cr^{6+} proportion. The effect of determining the background parameter values was less than ±3% units in all cases. Regarding the spectral parameters, the analysis result was found to be most sensitive to the assumed chemical shift between the two states. For

iron oxide the effect was ±4–10% units and for chromium oxide ±1–2% units; the "Seah" background showed the lowest sensitivity in both cases. Comparing these uncertainties to the effect of the background subtraction method, it can be concluded that the effect of the background choice is at least as strong as that of the typical sources of uncertainty.

In a general comparison between the Shirley and Tougaard backgrounds, the Tougaard background has been found to be better [6,7]. Thus, it could be stated that a Tougaard-type background should be used also in the chemical state quantification if a compatible lineshape can be found. The results of this work show that such a lineshape for iron and chromium oxides is a Gaussian–Lorentzian product function with a constant–exponential tail (Eqs. (7)–(9)).

Regarding the chemical analysis, the primary criterion for a background would be that after it has been subtracted, the correct quantification result is obtained. Naturally, the background cannot be considered alone but rather together with the used lineshape. In this work, the surface composition was not known exactly, but all the studied methods gave a result that is in agreement with the bulk stoichiometry of iron oxide and UV–Vis results for chromium oxide. Thus, when comparing the performance of the backgrounds, we have to use secondary criteria, such as the chi-square value of the fit, the obtained 2p intensity ratio, and the sensitivity of the analysis for assumptions concerning the spectral parameters. None of the backgrounds can be regarded as the best in all the studied cases, but some common trends can be seen. The "Seah" background seems to be least sensitive to the assumptions on the chemical shift and binding energy referencing, and for four out of five analyzed spectra "Seah" gave the lowest chi-square value. By these arguments, the "Seah" background could be recommended for the chemical quantification provided that the lineshape is the same as used here.

Limiting the analysis of iron and chromium oxide spectra to the $2p_{3/2}$ peak instead of the entire 2p region was observed to change the result of the state quantification in particular if a symmetric lineshape was used.

References

[1] D.A. Shirley, Phys. Rev. B 5 (1972) 4709.
[2] S. Tougaard, Surf. Interface Anal. 11 (1988) 453.
[3] S. Tougaard, Surf. Interface Anal. 25 (1997) 137.
[4] M.P. Seah, I.S. Gilmore, S.J. Spencer, Surf. Sci. 461 (2000) 1.
[5] M.P. Seah, Surf. Sci. 420 (1999) 285.
[6] S. Tougaard, C. Jansson, Surf. Interface Anal. 20 (1993) 1013.
[7] C. Jansson, et al., Surf. Interface Anal. 23 (1995) 484.
[8] C.-U. Ro, J. Korean, Chem. Soc. 39 (1995) 617.
[9] P.M.A. Sherwood, J. Vac. Sci. Technol. A 14 (1996) 1424.
[10] S.M.K. Airaksinen, A.O.I. Krause, J. Sainio, J. Lahtinen, K.-J. Chao, M.O. Guerrero-Pérez, M.A. Bañares, Phys. Chem. Chem. Phys. 5 (2003) 4371.
[11] P.J. Cumpson, M.P. Seah, Surf. Interface Anal. 18 (1992) 345.
[12] J.E. Castle, A.M. Salvi, J. Electron. Spectrosc. Relat. Phenom. 114–116 (2001) 1103.
[13] J.E. Castle, A.M. Salvi, J. Vac. Sci. Technol. A 19 (2001) 1170.
[14] S. Tougaard, Solid State Commun. 61 (1987) 547.
[15] C. Scharfschwerdt, J. Kutscher, F. Schneider, M. Neumann, S. Tougaard, J. Electron. Spectrosc. Relat. Phenom. 60 (1992) 321.
[16] S. Tougaard, Surf. Sci. 216 (1989) 343.
[17] S. Doniach, M. Šunjić, J. Phys. C 3 (1970) 285.
[18] R.P. Gupta, S.K. Sen, Phys. Rev. B 12 (1975) 15.
[19] N.S. McIntyre, D.G. Zetaruk, Anal. Chem. 49 (1977) 1521.
[20] A.P. Grosvenor, B.A. Kobe, N.S. McIntyre, S. Tougaard, W.N. Lennard, Surf. Interface Anal. 36 (2004) 632.
[21] T. Fujii, F.M.F. de Groot, G.A. Sawatzky, F.C. Voogt, T. Hibma, K. Okada, Phys. Rev. B 59 (1999) 3195.
[22] T. Droubay, S.A. Chambers, Phys. Rev. B 64 (2001) 205414.
[23] E. Ünveren, E. Kemnitz, S. Hutton, A. Lippitz, W.E.S. Unger, Surf. Interface Anal. 36 (2004) 92.
[24] S.J. Roosendaal, I.A.M.E. Giebels, A.M. Vredenberg, F.H.P.M. Habraken, Surf. Interface Anal. 26 (1998) 758.
[25] P. Graat, M.A.J. Somers, Surf. Interface Anal. 26 (1998) 773.
[26] P.M.A. Sherwood, Data analysis in XPS and AES, in: D. Briggs, M.P. Seah (Eds.), Practical Surface Analysis, Vol. 1, Auger and X-ray Phototoelectron Spectroscopy, second ed., John Wiley & Sons, Inc., 1990, p. 555.
[27] N. Fairley, in: D. Briggs, J.T. Grant (Eds.), Surface Analysis by Auger and X-ray Photoelectron Spectroscopy, IM Publications and Surface, Spectra Limited, 2003, p. 397.
[28] J.H. Scofield, J. Electron. Spectrosc. Relat. Phenom. 8 (1976) 129.
[29] R. Nyholm, N. Mårtensson, A. Lebugle, U. Axelsson, J. Phys. F 11 (1981) 1727.
[30] C.J. Powell, M.P. Seah, J. Vac. Sci. Technol. A 8 (1990) 735.

[31] C.S. Kuivila, J.B. Butt, P.C. Stair, Appl. Surf. Sci. 32 (1988) 99.
[32] S. Tougaard, Appl. Surf. Sci. 100/101 (1996) 1.
[33] S. Tougaard, QUASES, Version 5.0, Software for Quantitative XPS/AES of Surface Nano-Structures by Analysis of the Peak Shape and Background, 2002.
[34] S.J. Roosendaal, B. van Asselen, J.W. Elsenaar, A.M. Vredenberg, F.H.P.M. Habraken, Surf. Sci. 442 (1999) 329.
[35] E.R. Malinowski, Factor Analysis in Chemistry, second ed., John Wiley & Sons, Inc., 1991.